Dynamic Light Scattering and Viscosity Studies on the Association Behavior of Silicone Surfactants in Aqueous Solutions

Saurabh S. Soni, Nandhibatla V. Sastry,* and John George

Department of Chemistry, Sardar Patel University, Vallabh Vidyanagar−388 120, Gujarat, India

H. B. Bohidar

School of Physical Sciences, Jawaharlal Nehru University, New Delhi−110 067, India

Received: November 12, 2002; In Final Form: February 5, 2003

The micellar structure of three nonionic amphiphilic silicone surfactants based on polyether-modified poly(dimethylsiloxane) has been investigated by dynamic light scattering (DLS) and viscosity measurements. Out of these three, two surfactants have a comblike structure, and one has a trisiloxane-type structure with a linear poly(dimethylsiloxane) backbone chain and a grid containing block oligomers of oxyethylene and/or oxypropylene attached to one of the units as grafts. The dilute-solution phase diagram of the trisiloxane surfactant has been constructed and explained. The hydrodynamic radius, R_h, and the size distribution in terms of the translational diffusion coefficient of the micelles were obtained from the analysis of the time correlation function of the scattering intensity measured at a fixed scattering angle of 90° and for different concentrations and temperatures (30, 45, and 60 °C). The micellar systems under study were found to have a less polydisperse size distribution. The analysis of DLS data revealed the presence of oblate ellipsoidal micelles that showed continuous growth along the semimajor axis, *b*, with the rise in temperature. The values of the mass average association number, the hydrodynamic expansion factor, and the intrinsic viscosity of the micelles exhibited a similar temperature dependence, but the dominant repulsive solute (hydrophobic part)−solvent interactions noticed at 30 °C were found to get weaker. The combination of small-angle neutron scattering (SANS), DLS data, and intrinsic viscosities of micellar solutions were used to estimate the hydration of the micelles. The observed unusual temperature dependence of the micellar hydration has been explained.

1. Introduction

Amphiphilic polymers containing hydrophobic and hydrophilic moieties have been extensively studied for their surfactant properties. The molecular architectures of these polymers can be tailored to suit a specific application. The choice of hydrophilic moiety invariably has been poly(oxyethylene), E_n because of (i) its excellent water solubility up to 100 °C and (ii) its usefulness in easily synthesizing polymers with a wide range of molecular weights.[1] The hydrophobic parts of these polymers have been either poly(oxypropylene), P_n, poly(oxybutylene), B_n, polystyrene, S_n, or polyisobutylene, IB_n, and so forth. Of all of these, the diblock E_nP_m, E_nB_m, S_nE_m and triblock $E_nP_mE_n$ and $E_nB_mE_n$ ($P_nE_mP_n$ and $B_nE_mB_n$) copolymers have attracted great attention, and all these copolymers are now commercially available. The surfactant properties—especially the surface activity, self-association, and phase behavior of these copolymers—have been extensively measured. The association behavior has been monitored using several experimental methods, and the results of such studies are reviewed by Chu and Zhou,[2] Almgren et al.,[3] Alexandridis,[4] and Booth and Attwood.[5] One of the main disadvantages of the above-mentioned polymeric surfactants has been that these are less effective or sometimes fail in organic media. To make available polymeric surfactants, which are effective both in aqueous and nonaqueous media, silicone surfactants, a generic name given to molecules consisting of a permethylated siloxane group joined to one or more polar groups, have been synthesized. A recent volume of the Surfactant Science Series[6] has reviewed the synthetic methods and surface-active and phase-behavior studies along with various novel applications areas such as stabilizers for polyurethane foam, deemulsifiers in oil production, and defoamers in fuels of silicone surfactants. A more recent paper[7] describes the utility of silicone surfactants in other industrial formulations such as inks, paints and coatings, textiles, agriculture, and personal care products. Besides the above-mentioned industrial importance, silicone surfactants are interesting from an academic point of view because by using different synthetic routes molecular architectures of different types and of a wide range of molecular weights can be generated.[6−9] The polar groups in silicone surfactants can be either nonionic (poly(oxyethylene) (POE), poly(oxyethylene) (POE)/poly(oxypropylene) (POP), or carbohydrates), anionic, or cationic as well as zwitterionic. The molecular architectures range from graft type (with a central poly(dimethylsiloxane) (PDMS) chain with a grid of POE−POP grafted into it) to ABA block type (where A = POE and B = PDMS) to trisiloxane (linear, branched, or cyclic) with three DMS units to one of which a POE chain is attached. The literature reveals that despite the wide and extensive use of silicone surfactants little is known about their association behavior in water in general and the physical and geometrical characteristics of their associates in

* To whom correspondence should be addressed. E-mail: nvsastry_ad1@sancharnet.in.

10.1021/jp027444x CCC: $25.00
Published on Web 05/02/2003

CHART 1: General Structure of Silicone Surfactants.

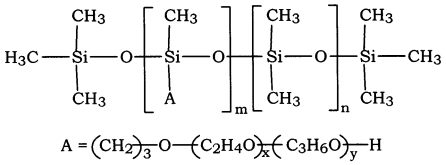

particular. Systematic and detailed investigations of the characterization of micelles formed by well-defined silicone surfactants and the influence of various factors such as temperature, molecular architecture, and additives on the micellar structures are highly desirable and will establish a possible correlation between micellar architecture and specific applications.

Gradzielski et al.[10] have monitored the association behavior of tri- and polysiloxane surfactants by using static light scattering and small-angle neutron scattering (SANS) methods both in dilute and concentrated aqueous solutions. It has been concluded by the authors that both types of silicone surfactants formed globular micelles, whose size hardly changed in the concentration range of 1−20% (w/v) at 25 °C. We have recently reported[11] systematic investigations on cloud points, surface activity, SANS, and viscosity measurements on aqueous solutions of two comblike polyether-modified poly(dimethylsiloxanes). Model fitting of SANS data showed that (i) both of the surfactants formed oblate ellipsoidal micelles with a constant size (in the concentration range of of 1−5% (w/v)) and (ii) the micelles registered a 30−60% increase in size along the semimajor axis with a similar rise in the association number and the other micellar parameter (i.e., the number density of micelles changed inversely with the rise in temperature). The changes in the micellar size and other parameters have been interpreted mainly in terms of dehydration effects at elevated temperatures as observed from the viscosity data. We could not ascertain information on the hydration water within associates, the micellar size distribution, and intermicellar interactions from our SANS analysis.

Therefore, to characterize the micelles of these silicone surfactants fully, we report a detailed study on dynamic light scattering (DLS) and viscosity measurements on aqueous solutions of two comblike polyether-modified poly(dimethylsiloxanes) and one trisiloxane surfactant at different concentrations and temperatures. DLS data are analyzed to extract various useful micellar parameters, and an attempt has also been made to combine the structural information emanating from DLS, SANS, and viscosity measurements.

2. Experimental Section

2.1. Materials. The silicone surfactants were obtained as gift samples from Th. Goldschmidt AG, Germany. They are polyether-modified poly(dimethylsiloxanes). The general structure of silicone surfactants is shown in Chart 1.

Values of *m* and *n*, which represent the polyether-modified hydrophilic methyl siloxane and hydrophobic poly(dimethylsiloxane) units and the values of *x* and *y* that denote the number of oxyethylene and oxypropylene units in the polyether grid[12] are summarized in Table 1. Surfactant SS-3 thus has a branched trisiloxane structure. It can be seen that the hydrophilicity of these surfactants is due to *x* units of oxyethylene (OE) in a given sample. These products are of commercial origin with *m*, *n*, *x*, and *y* being average numbers, and the branch group A is statistically distributed over the silicone chain. The surfactants were used as received without any further purification.

TABLE 1: Molecular Parameters, Number of Polyether-Modified Siloxane, *m*, Poly(dimethylsiloxane), *n*, Oxyethylene (OE), *x*, and Oxypropylene (OP), *y*, Units and Molar Mass of Silicone Surfactants

silicone surfactant	*m*	*n*	*x*	*y*	% EO	molar mass g mol^{-1}
SS-1	5	13	12	0	100	4360
SS-2	5	20	10	4	75	5600
SS-3	1	0	12	3	80	980

Water, freshly distilled from an all-Pyrex glass still, was used in preparing stock solutions (of 10 wt % (w/v)) in stoppered glass vials.

2.2. Methods. The dilute-solution phase diagram has been constructed by reproducible visible observation following warming and cooling cycles. The surface tension of the surfactant solutions was measured by the drop-weight method using a modified stalagmometer.[13]

The light-scattering apparatus consisted of a laboratory goniometer with two arms. One of these arms housed the excitation source, which was a solid-state frequency-doubled Nd:YAG laser radiating at a wavelength of 532 nm. The DLS experiments were carried out at a fixed scattering angle of 90°. The other arm of the goniometer had the photomultiplier tube mounted onto it, enabling the angle-dependent detection of scattered light. Surfactant solutions were ultracentrifuged at ∼10 000 rpm for about half an hour and were then directly loaded into optical-quality 5-mL borosilicate cells and sealed. Each cell was then held inside a homemade temperature controller.[14] This controller provided temperature regulation in the range of 15−75 °C with an accuracy of ±0.1 °C. Scattered light from the sample solutions was detected by the photomultiplier tube, and the photocurrent was suitably amplified and digitized before it was fed to a 1024-channel digital correlator (Brookhaven Instruments Inc., model BI-9000AT). The whole scattering apparatus was placed on a vibration isolation table (Newport Corp.). The correlation spectra were recorded at different temperatures. In all of the experiments, the difference between the measured and calculated baselines was not allowed to go beyond ±0.1%. The data that showed an excessive baseline difference were rejected. All of the data exhibited a single narrow distribution. The unimodal particle sizes were determined through the CONTIN[15−17] software provided by the Brookhaven Instrument Company.

The flow times of surfactant solutions and water were obtained by using Ubbelohde suspended-level viscometers. Two viscometers were used to record flow times in the range of 130−360 s, thus avoiding any kinetic corrections. Shear corrections were not taken into consideration because the obtained intrinsic viscosities were always less than 3 dL g^{-1}. The flow volume was greater than 5 mL, making drainage corrections unimportant. Viscometers were suspended in ISREF (India) thermostatic water baths maintained at a constant temperature that was accurate to ±0.01 °C.

The densities of aqueous surfactant solutions were measured by using a high-precision Anton Paar density meter (DMA 5000). The measured densities are accurate to ±0.000001 g cm^{-3}, and the temperature during the measurements has a stated precision of ±0.001 °C.

DLS Data Analysis. A DLS (dynamic light scattering) experiment measures the time correlation function $g_2(t)$ of the scattering intensity $I(t)$ at a given q defined by[18]

$$g_2(t) = \frac{\langle I(t')\, I(t'+t)\rangle}{\langle I(t')\rangle^2} \qquad (1)$$

which is related to the scattering-field autocorrelation function $g_1(t)$ by the Siegert relation[19]

$$g_2(t) = A + B|g_1(t)|^2 \tag{2}$$

where A defines the baseline of the correlation function as

$$|g_2(t)|_{t\to\infty} = A \tag{3}$$

and B is the spatial coherence factor. The ratio $^B/_A$ is the signal modulation, and better data quality demands $^B/_A \geq 50\%$.

For solutions containing particles undergoing Brownian motion (i.e., polymer or colloidal solutions), the field autocorrelation function $g_1(t)$ is given as

$$g_1(t) = \sum_i A_i \exp(-\Gamma_i t) \tag{4}$$

where Γ_i is the relaxation frequency that characterizes various relaxation modes that include relaxations due to the translational diffusion, rotational diffusion, bending modes, and so forth. The relative mode strength (amplitude) of the ith relaxation mode is A_i. For the present case, center-of-mass diffusion is the dominant process, and Γ_i has been identified as $\Gamma_i = D_i q^2$, where the translational diffusion coefficient of the ith micelle is D_i, the scattering vector $q = (^{4\pi n}/_{\lambda}) \sin(^{\theta}/_2)$, n is the refractive index of the solution, θ is the scattering angle, and λ is the wavelength of light source in the medium. The expression for $g_1(t)$ remains valid for polydisperse samples and for situations where the relaxation frequency distribution has several peaks. In the present situation, the micellar solutions were highly polydisperse. The correlation data were force fitted to an effective single-exponential relaxation using the CONTIN algorithm. The fitting of double or multiexponential relaxations did not yield acceptable χ^2 values. However, CONTIN provided excellent data fitting with acceptable statistical accuracy. This analysis yielded the effective relaxation frequency Γ from which D was calculated. The normalized variance of Γ gave the effective polydispersity, P, values. Again, P and D are related to the micellar concentration, N_i, and molecular weight, M_i, as

$$\bar{D} = \frac{\sum_i D_i N_i M_i^2}{\sum_i N_i M_i^2} \tag{5}$$

Consequently, P can be defined as

$$P = \frac{\langle (D - \bar{D})^2 \rangle}{(\bar{D})^2} \tag{6}$$

Further details of this discussion can be found elsewhere.[19]

In dilute solutions, the concentration dependence of the translational average diffusion coefficient can be expressed adequately by a first-order expansion:

$$\bar{D} = \bar{D}_o(1 + k_D C) \tag{7}$$

$\bar{D}_o$ is the z-average diffusion coefficient at infinite dilution, and k_D is the diffusion second virial coefficient. According to the Einstein relation, the $\bar{D}_o$ is inversely proportional to the translational frictional coefficient, f_t, at infinite dilution by the relation

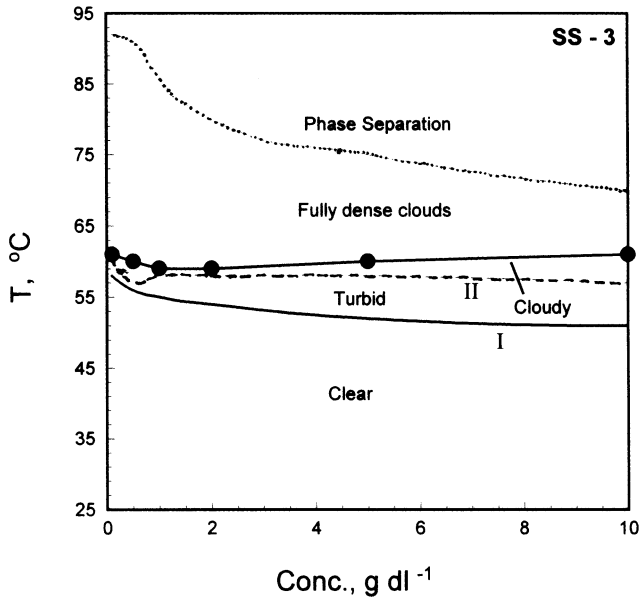

Figure 1. Phase diagram of trisiloxane silicone surfactant (SS-3) in aqueous solutions. Final cloud points (●).

$$\bar{D}_o = \frac{k_B T}{f_t} \tag{8}$$

where k_B is the Boltzmann constant and T is the absolute temperature. The value of f_t obtained via eq 8 can be used for a direct estimation of the hydrodynamic radius, R_h, of the micellar associates, provided that they have a spherical shape, using the relation $f_t = 6\pi\eta R_h$ per the Stokes law. Tanford[20] expressed the frictional coefficient for prolate and oblate ellipsoids of the revolutions of semiaxes b and a by

$$f_t = \frac{6\pi\eta b(1 - a^2/b^2)^{1/2}}{\ln\left[\dfrac{1 + (1 - a^2/b^2)^{1/2}}{a/b}\right]} \qquad \text{(prolate ellipsoid)} \tag{8a}$$

and

$$f_t = \frac{6\pi\eta a(b^2/a^2 - 1)^{1/2}}{\tan^{-1}(b^2/a^2 - 1)^{1/2}} \qquad \text{(oblate ellipsoid)} \tag{8b}$$

where b is the semimajor axis and a is the semiminor axis. The 3D shape is conclusively ascertained through independent measurements of the translational and rotational diffusivity of the scattering particle. This procedure has a maximum resolution and reliability in the depolarized scattering geometry. In addition, another approach was used to extract the same information, which will be discussed in section 3.3.1.

3. Results and Discussion

3.1. Dilute-Solution Phase Diagrams. The dilute-solution phase diagrams for SS-1 and SS-2 surfactants have been discussed previously.[11] The phase diagram for the SS-3 surfactant, as depicted in Figure 1, has similar features to those observed earlier for the other two surfactants.[11] The solutions in the concentration region of 0.1−10 wt % (w/v) remain initially clear over a temperature range of 54−57.5 °C and then

TABLE 2: Initial Turbidity and Final Cloud Points for Silicone Surfactant Aqueous Solutions

	SS-1		SS-2		SS-3	
concn g dL^{-1}	initial turbidity °C	Cp °C	initial turbidity °C	Cp °C	initial turbidity °C	Cp °C
0.1	75.5	85.0	63.5	69.0	58.0	61.0
0.5	78.0	83.5	62.5	66.0	56.5	59.5
1.0	68.0	79.0	61.0	64.0	55.0	58.5
2.0	64.0	77.0	62.0	65.0	53.0	59.0
5.0	55.0	81.0	50.0	66.5	52.5	60.0
10.0	58.0	84.5	51.5	68.5	51.0	62.0

become turbid and cloudy. The temperatures at which cloudiness appears uniformly in the solutions have been marked as cloud points and are shown as filled circles in the Figure. It was found that upon further warming the cloudiness becomes more dense with a visible phase separation beyond temperature limits marked by the upper dashed line in the Figure. The dilute-solution phase diagrams of SS-1 and SS-2 surfactants did not show any phase separation up to temperatures close to 95 °C. SS-3, because of its trisiloxane structure, has only one branch of the nonionic polar $(OE)_{12}$-$(OP)_3$ grid. Thus, it has fewer hydrophilic parts in comparison to several of them in SS-1 and SS-2. It was reasoned earlier by us that the oxyethylene part of the silicone surfactants contributes to the overall solubility in water up to the temperature range marked by curve I over the studied concentration range.[11] Because it is well known that poly(oxyethylene) homopolymers (with molecular weights of 10^2 to 10^5) do not exhibit any phase separation even at temperatures close to 100 °C, the appearance of turbidity in SS solutions between the temperature limit of curves I and II is mainly attributable to both dehydration and to a weakening of the miscibility of the silicone part at elevated temperatures. Our previous SANS measurements on SS-1 and SS-2 surfactant solutions further showed that micellar associates elongate by 30−60% along the semimajor axis, *b*, at temperatures close to the point at which solutions change from clear to turbid. Thus, the region of turbidity in the phase diagram marks the formation of micellar associates of a larger size, which grow further into particles of heavier mass in the cloudy region.

A comparison of initial turbidity and cloud points (Cp) for the three surfactants has been presented in Table 2. A perusal of the data reveals that the solutions of short-chain linear trisiloxane silicone surfactant SS-3 show turbidity and cloudiness at temperatures lower than those for the other graft or comblike counterparts of SS-1 and SS-2. Considering that the SS-3 surfactant has low molecular weight and a smaller percentage of OE content than SS-1 and SS-2 surfactants, the observed lower cloud points in the former can be attributed to the presence of less-hydrophilic groups in its short chain than in the comblike structures of the latter. This perhaps is also the reason for the worsened miscibility of SS-3 solutions at high temperatures, which leads to the macrolevel phase separation of predominantly hydrophobic SS-3 molecules.

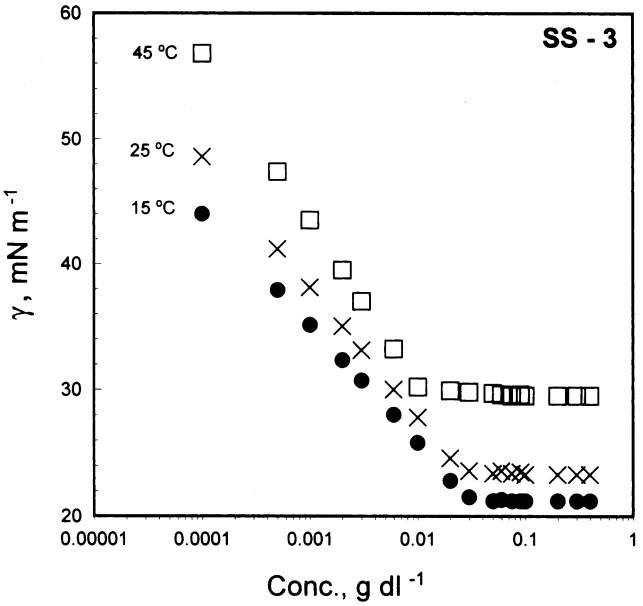

Figure 2. Plots of surface tension versus log(concentration) for SS-3 aqueous solutions at different temperatures.

3.2. Surface-Active Behavior. The values of critical micellar concentrations (CMC) of the SS-3 surfactant as extracted from surface tension−log concentration plots (Figure 2) along with various surface-active properties such as surface pressure, π_{CMC}, surface excess concentration, Γ_m, area per molecule at the air/water interface, a_1^s, surface tension at CMC, γ_{CMC} and the concentration at which the surface tension of water is reduced by 20 units, $C_{20,}$ are listed for 15, 25, and 45 °C in Table 3. The CMC values at different temperatures were further used to calculate the thermodynamic parameters, viz., the free energy, ΔG°_{mic}, enthalpy, ΔH°_{mic}, and entropy, ΔS°_{mic} of micellization. The same parameters are listed in the last three columns of the Table. The CMC values for the SS-3 surfactant are found to be always smaller than those for SS-1 and SS-2 surfactants at all three temperatures. For example, at 15 °C, CMC values for SS-1, SS-2, and SS-3 surfactants are 0.054, 0.047, and 0.033 g dL^{-1}, respectively. A similar trend was also observed at the other two temperatures. The remarkable feature of silicone surfactant micelles is that their CMC values show little variation with temperature. For example, the CMCs of SS-1, SS-2, and SS-3 are 0.054, 0.040, 0.025; 0.047, 0.034, 0.016; and 0.033, 0,025, and 0.010 g dL^{-1} at 15, 25, and 45 °C, respectively. Lin and Alexandridis[21] have also noted very small changes in CMC values (0.05 to 0.040 g dL^{-1} in the temperature range of 24 to 40 °C) for a silicone surfactant that has a similar structure to that of SS-1 and SS-2 but with a large number of dimethylsiloxane units. The comparison of γ_{CMC} and C_{20} values for SS-1 and SS-2 with the SS-3 surfactant revealed that SS-3 has a lower γ_{CMC} value (21.2 mN m^{-1}) than SS-1 (28.0 mN m^{-1}) and SS-2 (27.5 mN m^{-1}) and that C_{20} for SS-3 (9.6×10^{-6} g dL^{-1}) is lower than that for SS-1 (2.4×10^{-5} g dL^{-1}) and SS-2 ($5.6 \times$

TABLE 3: Parameters of the SS-3 Surfactant

temp °C	CMC g dL^{-1}	C_{20} g dL^{-1}	CMC/C_{20}	$\Gamma_m \times 10^{10}$ mol cm^{-2} [a]	a_1^s Å^2 [b]	γ_{CMC} mN m^{-1} [c]	π_{CMC} mN m^{-1} [d]	ΔG°_{mic} kJ mol^{-1}	ΔH°_{mic} kJ mol^{-1}	ΔS°_{mic} kJ K^{-1} mol^{-1} [e]
					SS-3					
15	0.033 ± 0.005	9.6×10^{-6}	3438	1.9 ± 0.2	89 ± 2	21.2 ± 0.2	52.2 ± 0.2	-28.8	26.2	0.19
25	0.025 ± 0.006	4.8×10^{-5}	522	1.8 ± 0.2	91 ± 2	23.6 ± 0.4	48.2 ± 0.4	-30.4	28.0	0.20
45	0.010 ± 0.005	4.0×10^{-4}	25	1.8 ± 0.1	93 ± 2	30.0 ± 0.3	38.6 ± 0.3	-34.9	31.9	0.21

[a] Surface excess concentration Γ_m. [b] Area per copolymer molecule a_1^s. [c] Surface tension at CMC γ_{CMC}. [d] Surface pressure π_{CMC}. [e] At different temperatures.

10^{-5} g dL^{-1}) at 15 °C. This shows that the SS-3 surfactant has to be more hydrophobic, more effective, and more efficient than the SS-1 and SS-2 surfactants. The short-chain trisiloxane surfactant (SS-3) adsorbs onto the air/water interface more tightly than its comblike counterparts, which have higher numbers of hydrophilic OE parts. This is indeed reflected in the estimated smaller a_1^s values for the SS-3 surfactant over the values for the other two. (a_1^s values at 15 °C for SS-1, SS-2, and SS-3 are 129 ± 5, 106 ± 3 and 89 ± 2 Å^2.) Except for these differences, the micellization of all three surfactants is predominantly entropy-driven (positive values) because ΔH°_{mic} values were always positive. Gentle and Snow[22] and Hoffmann and Ulbricht[23] have also reported similar differences in surface-active parameters between short-chain trisiloxane and comblike silicone surfactants.

3.3. Association Behavior. To characterize the micelles of silicone surfactants further for the particle dispersity and hydration, DLS data have been treated in the following manner.

3.3.1. Micellar Shape and Size. The concentration dependence of average translational diffusion coefficients, $\bar{D}$, as obtained from eq 5 was expressed through eq 7 (see parts a−c of Figure 3 for the respective plots) to get the average translational diffusion coefficients at infinite dilution, $\bar{D}_o$. Our earlier SANS studies[11] conclusively proved that the associates of the two silicone surfactants used in this study are oblate ellipsoidal in shape with characteristic *a* and *b* values, so we explored the possibility of testing the self-consistency of the information obtained from two independent sets of SANS and DLS experiments in the following manner. We used a single constant value of *a* for the SS-1 and SS-2 surfactants (i.e., 23 and 25 Å from our earlier SANS data analysis) to calculate the frictional coefficients, f_t, with the help of eqs 8a and 8b, assuming prolate and oblate shapes for the micelles and for different initial trial values of *b*. This procedure yielded f_t values for different sets *a* and *b*. Our analysis revealed that f_t values calculated for the given set of *b* and *a* as listed in columns 5 and 6 of Table 4 and as applicable for oblate associates reproduced the DLS-determined $\bar{D}_o$ values of column 2 in Table 4. Because the SANS and DLS data analysis independently corroborate the fact that the micellar associates are oblate ellipsoidal in shape with mutually agreeable size parameters *b* and *a*, we state that polydispersity play a negligible role in the DLS data treatment. This is in fact the advantage of using the CONTIN algorithm.

3.3.2. Micellar Molar Mass and Association Number. The values of the semimajor and semiminor axes (*b* and *a*, respectively) for SS-1 and SS-2 micelles in D_2O were previously deduced from SANS intensities, considering the scattering from the hydrophobic core part only because we could not observe any contrast between the highly hydrated outer shell and the solvent D_2O.[11] Thus, the values of *a* and *b* probably represent the true dimensions of a dry core. Setting b^2a equal to R_o^3, where R_o is the radius of the dry core, the volume component can be related to[24]

$$\frac{4\pi R_o^3}{3} = \frac{\bar{v}\,\bar{M}_m}{N_A} \tag{9}$$

where $\bar{v}$ is the partial specific volume of micelles, $\bar{M}_m$ is the micellar molar mass, and N_A is Avogadro's number. Therefore, assuming an unsolvated micellar core and employing SANS values of unhydrated micellar axes of *a* and *b* and densitometrically estimated partial specific volume, $\bar{v}$, values, the micellar molar masses, $\bar{M}_m$, were calculated via eq 9. The mass-average association numbers, $\tilde{n}$, were then calculated from

$$\tilde{n} = \frac{\bar{M}_m}{\text{molar mass of surfactant molecule}} \tag{10}$$

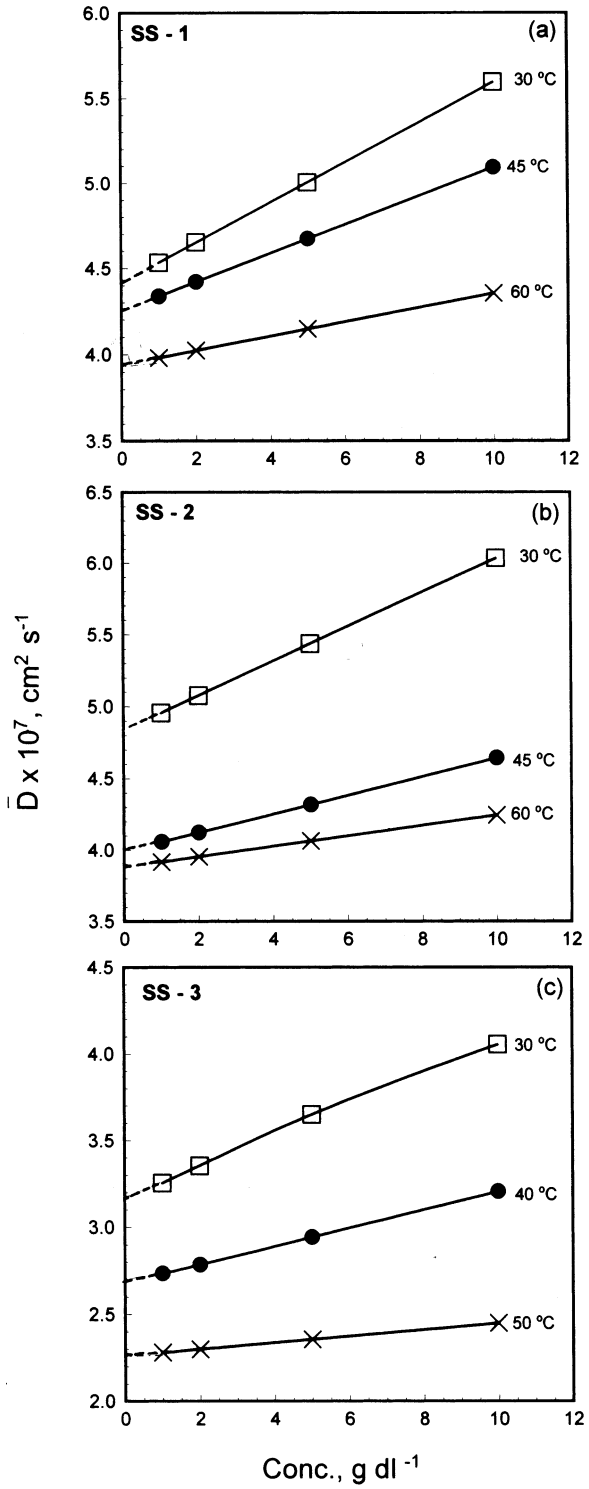

Figure 3. Plots of translational diffusion coefficient values versus concentration for (a) SS-1, (b) SS-2, and (c) SS-3 surfactant micelles at different temperatures.

The summary of the various micellar dimensions for SS-1, SS-2, and SS-3 micelles as extracted from the DLS data along with the micellar parameters on SS-1 and SS-2 micelles (from previous SANS measurements) is given in Table 4. Column four of the Table lists the values of the hydrodynamic radii, R_h,

TABLE 4: Parameters of Silicone Surfactant Ellipsoidal Micelles at Different Temperatures

	DLS								SANS[a]			
temp °C	$\bar{D}_o \times 10^7$ cm^2 s^{-1} [b]	P[c]	R_h[d] Å	b[e] Å	a[f] Å	b/a	$\bar{M}_m$[g] $\times 10^{-5}$ g mol^{-1}	$\tilde{n}$[h]	b[e] Å	a[f] Å	b/a	N[i]
					SS-1							
30	4.41 ± 0.15	0.28	63 ± 6	49 ± 3	25 ± 1	2.0	1.62 ± 0.10	37 ± 4	50	23	2.2	92
45	4.25 ± 0.10	0.32	92 ± 9	55 ± 3	25 ± 1	2.2	1.99 ± 0.13	46 ± 5	56	23	2.4	114
60	3.94 ± 0.18	0.28	130 ± 13	70 ± 4	25 ± 1	2.8	2.59 ± 0.15	60 ± 6	64	23	2.6	147
					SS-2							
30	4.84 ± 0.12	0.37	57 ± 6	43 ± 3	25 ± 1	1.7	1.63 ± 0.10	29 ± 3	48	25	1.9	45
45	3.99 ± 0.13	0.35	98 ± 10	58 ± 4	25 ± 1	2.3	1.86 ± 0.12	33 ± 3	53	25	2.1	54
60	3.88 ± 0.09	0.21	135 ± 14	80 ± 5	25 ± 1	3.2	3.64 ± 0.22	65 ± 7	75	25	3.0	107
					SS-3							
30	3.12 ± 0.06	0.51	71 ± 7	72 ± 4	20 ± 1	3.6	2.61 ± 0.16	266 ± 27				
40	2.68 ± 0.07	0.34	102 ± 10	108 ± 5	20 ± 1	5.3	5.69 ± 0.34	580 ± 58				
50	2.26 ± 0.05	0.24	171 ± 17	160 ± 8	20 ± 1	8.0	12.77 ± 1.28	1303 ± 130				

[a] For 2 wt % (w/v) solutions from reference 11. [b] Average translational diffusion coefficient at infinite dilution. [c] Polydispersity. [d] Hydrodynamic radius. [e] Semimajor axis. [f] Semiminor axis. [g] Micellar molar mass. [h] Mass-average association number. [i] Association number.

of micelles calculated from the experimentally derived f_t values as such. The R_h value thus has contributions from both the hydrophobic core and hydrophilic outer shell. The polydispersity, P, in associates was found to lie between 0.21 and 0.51. Hence, it can be concluded that the associates have lower polydispersity. As previously noted, the field autocorrelation function, $g_1(t)$, could be fit only to a single exponential (in the form of eq 4), and thus the associates have unimodal molecular weight distribution. This is in contrast to the bimodal size distributions in DLS intensities observed very recently for the micelles of a silicone surfactant of similar structure but with larger hydrophobic moieties[21] than the SS-1 and SS-2 surfactants.

However, the mass-average association number, $\tilde{n}$, as calculated from eq 10 and the association number, N, values derived from earlier SANS data were far different, and these differences are attributable to the different approaches used in the calculation. The $\tilde{n}$ value takes into account the total mass of the hydrophobic and hydrophilic parts of the single surfactant molecule. The N value was calculated by considering the micellar hydrophobic core volume and the volume of a hydrophobic unit in one surfactant molecule. Static light scattering data[25] on P-85 (a triblock $E_mP_nE_m$ copolymer) micelles in aqueous solutions gave an association number of 30, and SANS measurements[26] for the same copolymer micelles led to an N value of 116 at 25 °C. DLS and SANS data (columns 7 and 12, 9 and 13 of Table 4, respectively) show that the associates grow along the semimajor axis with a resulting increase in both $\tilde{n}$ and N values with the rise in temperature from 30 to 50 or 60 °C for the micelles of the three surfactants. The micellar growth can be explained by considering the dehydration, especially of hydrophobic core at elevated temperatures, and thus under these conditions associates can accommodate more surfactant molecules to fill the micellar space vacated by water molecules. A similar increase in micellar size and N values with the increase in temperature was also reported for several triblock copolymers of oxyethylene−oxypropylene−oxyethylene[2] and oxyethylene−oxybutylene−oxyethylene.[27] Another interesting feature of the data presented in Table 4 is that the associates of the SS-3 surfactant, which is a trisiloxane type, are bigger in size—large in terms of axial ratios—and accommodate more molecules. The value of the semimajor axis, b, is almost 2-fold greater over the same range for the micelles of other two comblike surfactants. The SS-3 surfactant has only one unit of D′ (with $(OE)_{12}$ and $(OP)_3$) flanked by one unit of M at each end. SS-1 and SS-2 have several D and D′ units and hence have a large number of $(OE)_x$ units along the branches, so it can be rationalized that the hydrophobic moieties of dimethylsiloxanes and oxypropylene units would acquire flat and compact conformations in micelles of trisiloxane surfactant, and the same attain perhaps a strained or coiled conformation because of the twisting needed to expose the hydrophilic branches to the aqueous environment in SS-1 and SS-2 micelles. The closeness of the molecules in the core of the micelles of the former type of surfactant yields larger associates with bigger $\tilde{n}$ values. A recent paper[21] considered the SANS analysis of 1 wt % (w/v) solutions of $MD_{70}D'_5$−RM with R = $-(CH_3)_2O-(OE)_{19}-(OP)_6-H$. The authors have treated the data in terms of spherical micelles at 25 °C and have reported an N value of 142 ± 6, which is much larger than for the micelles of the SS-1 and SS-2 surfactants used in the present study. Thus, it can be stated that surfactants with smaller ratios of hydrophilic to hydrophobic parts tend to form larger micelles with larger association number. There are few reports in the literature dealing with structural information on micelles of silicone surfactants in aqueous solutions. More studies are needed to validate our generalization. Gradzielski et al.[10] have estimated the micellar dimensions for a series of such surfactants with the general structure of M−D−D′R−M, where M = $Me_3SiO_{1/2}$, D = $-Me_2SiO-$, D′ = Me(R)SiO, and R = $-(CH_3)_2O-(OE)_x-(OP)_y-H$, using static light scattering (SLS) and SANS measurements. Our SS-1 surfactant has the same comblike molecular structural characteristics ($D_{13}D'_5EO_{12}$) as that of CL 681 in Gradzielski et al.[10] The authors assumed a spherical shape for the micelles and reported a dry micellar radius of 42.7 Å and an association number of 48 from SLS measurements. The micelles of another comblike surfactant with $D_{18}D'_5EO_{12}$ (CL 680) were also characterized by SANS, assuming a hard-sphere shape. This analysis of SANS curves in 2 wt % (w/v) solution at 25 °C yielded a hard-core radius of 42.6 Å, a hard-sphere interaction radius of 50.5 Å, and an association number of 56. Similarly, SANS analysis of a 1 wt % (w/v) solution of trisiloxane surfactant with 16 (OE) units gave an association number of 154 for spherically shaped micelles of 32.5-Å radius. The authors further noted that the estimated core radii of micelles were far larger than the length of the hydrophobic siloxane chains, and hence they suspected that micelles may not exist exactly in a spherical shape but as ellipsoids with an axial ratio close to unity.

In ref 21, Lin and Alexandridis have also not considered the ellipsoidal shape for the micelles of a comblike surfactant with long hydrophilic chains in treating their SANS data at 20 and

TABLE 5: Interaction Parameter k_D, Huggins Constant k_H, and Intrinsic Viscosity [η] for Silicone Surfactant Micelles at Different Temperatures

	SS-1			SS-2			SS-3		
temp °C	k_D mL g^{-1}	k_H	[η] dL g^{-1}	k_D mL g^{-1}	k_H	[η] dL g^{-1}	k_D mL g^{-1}	k_H	[η] dL g^{-1}
30	2.67	1.98	0.029	2.48	1.75	0.048	3.11	2.56	0.053
35		1.72	0.031		1.59	0.044		1.72	0.075
40		1.60	0.032		1.40	0.057	1.94	1.52	0.087
45	1.98	1.49	0.033	1.63	1.21	0.058		1.08	0.121
50		1.28	0.035		1.03	0.061	0.83	0.60	0.156
51.5								0.30	0.168
55		1.12	0.038		0.89	0.062			
60	1.05	0.92	0.041	0.95	0.73	0.064			
60.5					0.60	0.066			
62.5		0.72	0.043						

25 °C. But the authors did notice the growth of spherical micelles into an ellipsoidal shape at elevated temperature of 60 °C.

3.3.3. Micellar Interactions. The term k_D obtained from the slope of the linear plots of $\bar{D}$ and surfactant concentration (as per eq 7) is a measure of net interactions in the micelles due to thermodynamic and hydrodynamic factors. k_D in fact is related[28] to the thermodynamic second virial coefficient, A_2, and the frictional coefficient, f_t, through the relation $k_D = 2A_2\bar{M}_w - f_t - \bar{v}$, where $\bar{M}_w$ and $\bar{v}$ are the micellar molar mass and partial specific volume, respectively. The overall contribution of f_t to k_D can be ignored because these micelles are compact with a very small spatial extension. Thus, the sign of k_D depends only on the sign of A_2, which in turn depends on the intermicellar interactions. The values of k_D for SS-1, SS-2, and SS-3 surfactant micelles at different temperatures are listed in Table 5. It is clear that k_D values are always positive but become smaller in magnitude with increasing temperature, implying reduced intermicellar repulsions at elevated temperatures. Consequently, the k_D values for the SS-2 and SS-3 micelles fall below unity at elevated temperatures, just above which the solutions turn turbid. Also listed in the Table are values of the Huggins' constant, k_H, and the intrinsic viscosity, [η], as derived from the fits of reduced viscosities and surfactant concentration (Figure 4) following Huggins' relation: $\eta_{sp}/C = [\eta] + k_H[\eta]^2C$. The values of k_D and k_H agree in sign and show a similar decrease with the temperature. The positive values of k_D and k_H indicate pronounced repulsive interactions between the hydrophobic parts of the solute and solvent at room temperature. With the rise in temperature, this repulsive interaction is weakened, as reflected in the sharp decrease in k_D and k_H values. Thus, at elevated temperatures, solute−solute interactions (i.e., intermicellar attractive interactions) dominate; consequently, the micelles grow in size, and the association number and number density of micelles increase. The continuous rise in [η] values, which measures the hydrodynamic volume of micelles, also strongly supports the micellar growth.

3.3.4. Hydrodynamic Swelling Factor and Hydration. The hydrodynamic swelling factor, δ_h, is defined as

$$\delta_h = \frac{v_h}{v_a} \tag{11}$$

where v_h is the average hydrodynamic volume (i.e., $v_h = {}^4/_3\pi R_h^3$) and v_a is the average anhydrous volume of the micelles. v_a is calculated from $\bar{M}_m/N_A\rho$, where $\bar{M}_m$ is the average micellar molar mass, N_A is Avogadro's number, and ρ is the anhydrous density of the surfactants (1.0593 for SS-1, 1.0352 for SS-2, and 1.0135 g cm^{-3} for SS-3). The values of δ_h for the micelles

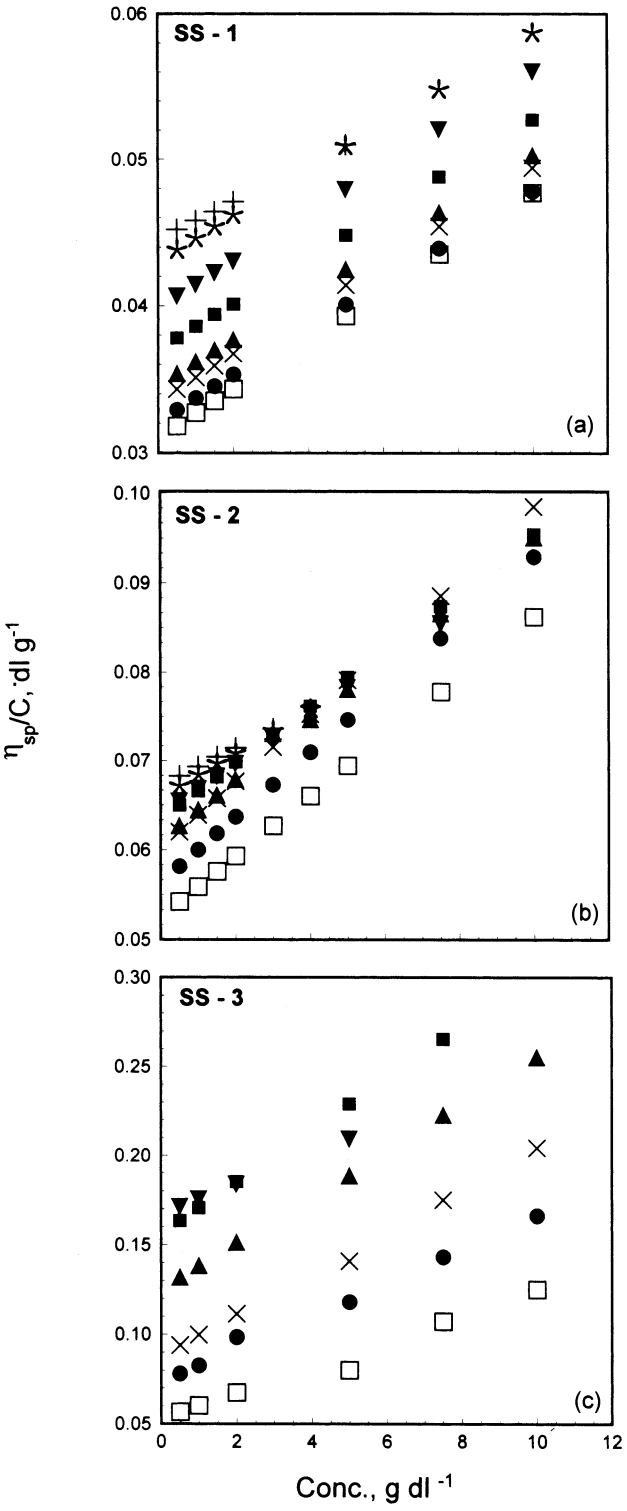

Figure 4. Plots of reduced viscosities versus concentration for (a) SS-1, (b) SS-2, and (c) SS-3 surfactant micelles at temperatures of (□) 30, (●) 35 °C, (×) 40 °C, (▲) 45 °C, (■) 50 °C, (a) (▼) 55 °C, (∗) 60 °C, (+) 62.5 °C, (b) (▼) 55 °C, (∗) 60 °C, (+) 60.5 °C, and (c) (▼) 51.5 °C

of the three surfactants at different temperatures are listed in column two of Table 6. The δ_h values show about a 3-fold increase at elevated temperatures.

The utility of having DLS and SANS data on the micelles of the same surfactants is that one can get a clear idea of the hydration of the micelles and the changes in it due to increasing temperature. By converting the micellar volume of ellipsoidal micelles estimated from ${}^4/_3\pi b^2 a$ (a and b values are taken from

TABLE 6: Hydrodynamic Swelling Factor, δ_h, and Number of Water Molecules Per OE Group, n_w, of Silicone Surfactant Micelles at Different Temperatures

temp °C	δ_h	n_w
	SS-1	
30	2.8 ± 0.3	4.3
45	3.3 ± 0.3	6.4
60	5.0 ± 0.5	12.2
	SS-2	
30	2.5 ± 0.3	7.0
45	3.8 ± 0.4	13.9
60	7.2 ± 0.7	22.8
	SS-3	
30	3.5 ± 0.4	8.5
40	4.7 ± 0.5	14.3
50	10.0 ± 1.0	38.4

columns 10 and 11 of Table 4 for SS-1 and SS-2 surfactants and columns 5 and 6 for the SS-2 surfactant), that of an equivalent sphere of radius R_o, the number of average water molecules per EO unit can be calculated in the following manner.

Assigning a mean volume v_{OE} (i.e. ,73.1 Å^3) per each OE unit and considering that the poly(oxyethylene) chain is evenly distributed throughout the shell region, the volume of the hydrophilic shell of the micelles, V_s, can be calculated from

$$V_s = \frac{4}{3}\pi(R_h^3 - R_o^3) = n\tilde{n}v_{OE} \qquad (12)$$

where n is the total number of OE units in a surfactant molecule, $\tilde{n}$ is the mass-average association number, R_h is the hydrodynamic radius (taken from column 4 of Table 4), R_o is the radius of the hydrophobic core, and v_{OE} is the mean volume of an OE unit in the hydrophilic shell. Taking values of 52 Å, 63 Å, 37, and 60 for the R_o, R_h, $\tilde{n}$, and n parameters for SS-1 surfactant micelles at 30 °C, respectively, the value of v_{OE} estimated using eq 12 is 206.5 Å^3. This value is about three times larger than the volume of one dry OE unit (i.e., 73.1 Å), so there is a strong indication that the POE chains in the shell have an open structure, leading to the trapping of several water molecules in addition to the hydration water. The chain length of POE (probably in a random coil conformation) in such an open structure can be estimated by the following equation:[29]

$$\langle r^2\rangle^{1/2} = \alpha(nC_N)^{1/2}l$$

$\langle r^2\rangle^{1/2}$ is the root-mean-square end-to-end distance, n is the number of bonds along the chain, α is the chain expansion factor (taken as 1.5), C_N is the swelling factor (numerically equal to 4), and l is the length of C−C and C−O bonds. The calculated $\langle r^2\rangle^{1/2}$ values for the POE parts of SS-1, SS-2, and SS-3 surfactants are 29, 27, and 29 Å, respectively, and are close to the ($R_h - R_o$) values of 24, 21, and 24 Å. Thus, the outer shell of the micelles is supposed to be filled with POE chains throughout its thickness.

Subtracting the volume of one dry OE unit from v_{EO} gives the volume occupied by water present in the shell. For SS-1 micelles, this leads to a 206.5 − 73.1 = 133.4 Å^3 hydration volume. Then, the number of water molecules, n_w, per OE unit in the shell can be estimated by the factor 133.4 Å^3/30 Å^3 (where 30 Å^3 is the volume of one water molecule). For SS-1 micelles, the n_w value is 4.3 at 30 °C. The values of n_w at different temperatures as calculated by the preceding procedure for the micelles of three surfactants are given in column three of Table 6.

A look at the temperature dependence of n_w interestingly reveals that it increases with the increase in temperature. This is rather surprising because one normally expects a decreasing trend because of the dehydration effects that are usually expected. It is worthwhile to note that at the maximum temperature of 60 °C the aqueous solutions of all three surfactants within the concentration range employed in DLS and viscosity measurements are clear. Thus, the POE segments still hold the surfactant micelles in water through hydrogen bonds, even though as mentioned earlier solute−solute interactions are predominant under these conditions. We propose the following explanation for the noted increase in the n_w values of the micelles at elevated temperatures. The oblate ellipsoidal micelles probably have a soft core (partially hydrated) because of the Si−O group bound water. Because the distinction between the hydrophobic core and the hydrophilic outer shell does not seem to be sharp, one would expect the presence of water in the core part just across the interfacial region between the two. A rise in the temperature shall thus initiate the expulsion of water consecutively from the core, interfacial region, inner part of the POE shell, and finally from the hydrophilic shell itself. Thus, as more water is expelled from the associates, more surfactant molecules enter into the associates (which leads to an increase in the association number, as explained earlier), and the hydrophobic chains stretch, causing the growth in the size of the micelles along the semimajor axis. Under the conditions of a clear-solution state, the hydrophilic outer shell is swollen more with the expelled hydrated water. Our proposed mechanism of micellar dehydration thus entails a preferential dehydration pattern as far as hydrophobic and hydrophilic portions of the micelles are concerned. Guo et al.[30] in fact observed from the deconvoluted FTIR spectra of the micelles of pluronic copolymer P-105 ($EO_{37}PO_{58}EO_{37}$) that even though both the PPO core and PEO outer shell undergo dehydration above 70 °C the PPO core was nearly anhydrous and the PEO corona still contained a substantial amount of water at the same temperature. Jain et al.[31] have also reported an increase in n_w values with increasing temperature for the pluronic F-88 ($EO_{37}PO_{58}EO_{37}$) micelles, as deduced from SANS measurements.

4. Conclusions

The nature of the dilute-solution phase diagram and the surface-active parameters for a short-chain trisiloxane silicone surfactant are different from that of poly(dimethylsiloxane)−graft−polyether copolymers. The total number of hydrophilic oxyethylene units in the polyether grid and the molecular architecture play critical roles in both the phase behavior and surfactant behavior of silicone surfactants. The presence of one graft of a polyether grid in a trisiloxane surfactant shifts the balance of the hydrophobic/hydrophilic ratio toward the former and hence decreases the CMC and area occupied by the molecule at the air/water interface. The CMC values of silicone surfactants in general show little variation in the temperature range of 15−45 °C. Otherwise, the micellization is found to be an entropy-driven process.

Dynamic light scattering (DLS) analysis shows that the micelles of silicone surfactants have a unimodal molecular weight distribution and lower polydispersity. The treatment of frictional coefficients at infinite dilution revealed that the silicone surfactants with their comblike molecular structure associate into oblate ellipsoidal micelles with characteristic axial $^b/_a$ ratios greater than 1. The micelles of the trisiloxane surfactant are much bigger and more asymmetric (with higher $^b/_a$ ratios) than

those of the other two comblike graft copolymers. The mass-average association number, $\tilde{n}$, for trisiloxane surfactant micelles has also been found to be 9- to 20-fold greater than for other two comblike surfactants. Thus, the trisiloxane surfactant with a simple structure and a lower hydrophobic/hydrophilic balance forms a compact, larger hydrophobic core of micelles and accommodates more surfactant molecules. The rise in temperature has a similar effect on the micelles of the three silicone surfactants, which grow along the semimajor axis with a concomitant increase in $\tilde{n}$ and the axial ratios. The growth of the micelles can be attributed to the possible expulsion of water from the interior of the micelles, causing the stretching of the hydrophobic core.

The combination of micellar effective core dimensions derived from SANS measurements, the hydrodynamic radius, R_h (which takes in to account the core and the outer corona shell), and the mass average-association number, $\tilde{n}$, was used to estimate the hydration of the micelles. The number of water molecules per OE unit, n_w, was found to lie between 4.3 and 8.5 at 30 °C for SS-1, SS-2, and SS-3 surfactant micelles. Interestingly, the n_w, values showed a gradual increase as the temperature was raised from 30 to 60 °C. This unusual temperature-dependent hydration needs to be accounted for properly. Because aqueous solutions of the three surfactants at 50 and 60 °C are clear and the hydrophilic oxyethylene part still holds the molecules in solution, it is thought that the micellar core could be soft (or partially hydrated). It is suggested that the rise in temperature can initiate a preferential dehydration from the inner micellar core and core−corona interface, so at elevated temperatures, asymmetric micelles with highly water-swollen coronas can be imagined. This replaces the repulsive interactions between the hydrophobic part of the solute and solvent (or water) with the solute−solute or intermicellar attractive interactions, as evidenced by the observed large decrease in the interaction parameters calculated from DLS and viscosity measurements.

Acknowledgment. S.S.S. thanks the IUC-DAEF, Mumbai, for granting a research assistantship under grant no. IUC/CRS-M-73/362-66.

References and Notes

(1) Piirma, I. *Polymeric Surfactants*; Surfactant Science Series; Marcel Dekker: New York, 1992; Vol. 42, Chapters 2 and 3, pp 17−84.

(2) Chu, B.; Zhou, Z. Physical Chemistry of Polyalkylene Block Copolymer Surfactants. In *Nonionic Surfactants*; Nace, V. M., Ed.; Surfactant Science Series; Marcel Dekker: New York, 1996; Vol. 60, p 67.

(3) Almgren, M.; Brown, W.; Hvidt, S. *Colloid Polym. Sci.* **1995**, *273*, 2.

(4) Alexandridis, P. *Curr. Opin. Colloid Interface Sci.* **1997**, *2*, 478.

(5) Booth, C.; Attwood, D. *Macromol. Rapid Commun.* **2000**, *21*, 501.

(6) *Silicone Surfactants*; Surfactant Science Series; Hill, R. M., Ed.; Marcel Dekker: New York, 1999; Vol. 86.

(7) Hill, R. M. Silicone (Siloxane) Surfactants. In *Encyclopedia of Physical Science and Technology* 3rd ed.; Meyers, R. A., Ed.; Academic Press: San Diego, CA, 2002; Vol. 14, p 793.

(8) Schafer, D. *Teside Surf. Detergents* **1990**, *27*, 154.

(9) Gruning, B.; Koerner, G. *Tenside Surf. Detergents* **1989**, *26*, 3.

(10) Gradzielski, M.; Hoffmann, H.; Robisch, P.; Ulbricht, W.; Gruning, B. *Tenside, Surfactants, Deterg.* **1990**, *27*, 366.

(11) Soni, S. S.; Sastry, N. V.; Aswal, V. K.; Goyal, P. S. *J. Phys. Chem. B* **2002**, *106*, 2607.

(12) Tegoprene-Silicone Surfactants Products; *Data and Information Technical Brochure*; Th. Goldschmidt, AG.: Essen, Germany, 1990.

(13) Jain, D. V. S.; Singh, S. *Indian J. Chem.* **1972**, *10*, 629.

(14) Bohidar, H. B.; Berland, T.; Jassang, T.; Fedex, J. *Rev. Sci. Instrum.* **1987**, *58*, 1422.

(15) Provencher, S. W. *Comput. Phys. Commun.* **1982**, *27*, 213.

(16) Provencher, S. W. *Comput. Phys. Commun.* **1979**, *27*, 227.

(17) Provencher, S. W. *Makromol. Chem.* **1979**, *180*, 201.

(18) Berne, B. J.; Pecora, R. *Dynamic Light Scattering*; Wiley: New York, 1976.

(19) Mazer, A. N. In *Dynamic Light Scattering*; Pecora, R., Ed.; Plenum Press: New York, 1985; pp 305.

(20) Tanford, C. *Physical Chemistry of Macromolecules*; Wiley: New York, 1961; pp 327.

(21) Lin, Y.; Alexandridis, P. *J. Phys. Chem. B* **2002**, *106*, 10845.

(22) Gentle, T. E.; Snow, S. A. *Langmuir* **1995**, *11*, 2605.

(23) Hoffmann. H.; Ulbricht, W. In *Silicone Surfactants*; Hill, R. M., Ed.; Surfactant Science Series; Marcel Dekker: New York, 1999; Vol. 86, Chapter 4, pp 97−136.

(24) Chu, B. *Laser Light Scattering*; Academic Press: New York, 1975; Chapter 8, pp 212−253.

(25) Brown, W.; Schillen, K.; Almgren, M.; Hvidt, S.; Bahadur, P. *J. Phys. Chem.* **1991**, *95*, 1850.

(26) Mortensen, K.; Pedersen, J. S. *Macromolecules* **1993**, *26*, 805.

(27) Yu, G.-E.; Yang, Y.-W.; Yang, Z.; Attwood, D.; Booth, C.; Nace, V. M. *Langmuir* **1996**, *12*, 3404.

(28) Vink, H. *J. Chem. Soc., Faraday Trans. 1* **1985**, *81*, 1725.

(29) Fried, J. R. *Polymer Science and Technology*; Prentice Hall: New York, 1995.

(30) Guo, C.; Liu, H. Z.; Chen, J. Y. *Colloid Polym. Sci.* **1999**, *277*, 376.

(31) Jain, N. J.; Aswal, V. K.; Goyal, P. S.; Bahadur, P. *J. Phys. Chem. B* **1998**, *102*, 8452.